frontiers | Frontiers in Physics

TYPE Original Research
PUBLISHED 15 February 2023
DOI 10.3389/fphy.2023.1098170

OPEN ACCESS

EDITED BY
Huan Yang,
Shandong University, China

REVIEWED BY
Yonggang Peng,
School of Physics, Shandong University, China
Hsin-Yu Ko,
Cornell University, United States

*CORRESPONDENCE
Zhi Zhu,
zhuzhi@usst.edu.cn
Yangmei Li,
sunberry1211@hotmail.com

SPECIALTY SECTION
This article was submitted to Atomic and Molecular Physics, a section of the journal Frontiers in Physics

RECEIVED 14 November 2022
ACCEPTED 30 January 2023
PUBLISHED 15 February 2023

CITATION
Sun T, Wang L, Hu R, Li Y and Zhu Z (2023), Light controls edge functional groups to enhance membrane permeability. *Front. Phys.* 11:1098170. doi: 10.3389/fphy.2023.1098170

Light controls edge functional groups to enhance membrane permeability

Tingyu Sun[1], Lei Wang[1], Rengkai Hu[1], Yangmei Li[2]* and Zhi Zhu[1]*

[1]Key Laboratory of Optical Technology and Instrument for Medicine, Ministry of Education, College of Optical-Electrical and Computer Engineering, University of Shanghai for Science and Technology, Shanghai, China, [2]Innovation Laboratory of Terahertz Biophysics, National Innovation Institute of Defense Technology, Beijing, China

Functionalized membranes have high potential value in a broad range of practical applications, and the functional groups at the membrane edge play a vital role in the permeability of the membranes. Here, based on an edge-functionalized graphene oxide (GO) membrane model, we theoretically report that high-frequency terahertz stimulation at the frequency near 44.0 THz can significantly enhance the water permeability of the membrane by nearly five times. Its mechanism was revealed to be that the stimulation amplified the C-O stretching of the functional groups and suppressed other vibration modes of the groups. As a result, the modulation of edge functional groups brings down the energy barricade of the membrane and allows water molecules to penetrate the GO membrane more easily. These findings provide a new perspective for enhancing membrane permeability by modulating particular functional groups such as the carboxyl on the edge of the GO membrane.

KEYWORDS

graphene oxide, terahertz light, spectrum, permeation enhancement, absorption

Introduction

Membranes play an imperative role in life science and industrial applications, such as disease treatment and water purification [1, 2]. It is of important significance to understand and manipulate the transportation of water through membranes in many physical, chemical, biological, and technical applications. In different artificial and biological membranes, functional groups on the membrane determine the properties of the membrane and have a great influence on the permeability of water [3]. For example, as a two-dimensional (2D) material derived from graphene, GO has almost completely different properties from graphene [4, 5]. Compared to hydrophobic graphene, the polar oxygen-containing functional groups on the membrane make it hydrophilic and have different properties from graphene in many ways [6, 7]. GO membranes, as a feasible artificial membrane for water desalination and wastewater treatment [8–10], was first developed by Nair et al., and it was discovered that stacking GO film can selectively block the motion of non-aqueous solutions and allow water permeation through a unique pathway [11]. From then, many attempts to develop the application of GO membrane and methods to control the interlayer spacing of stacking GO have been discovered [12–15].

The interlayer spacing of the stacking GO membrane determines the ion and water permeation efficiency, a smaller interlayer spacing leads to better ion-sieving performance, while the flow rate of water decreases exponentially with the reduction in interlayer spacing [16–20]. The carboxyl group at the edge of the GO membrane is one of the major factors affecting the permeation of water molecules and other ions through the membrane due to the steric effect [21–24]. Previous attempts made to enhance the permeability of GO were mainly surface modification or reassembling [25, 26]. In contrast, THz electromagnetism (EM)

stimulus is a novel and efficient approach. In recent years, the application of THz EM waves in biochemistry and the theoretical discussion on the interaction between light and matter are increasing gradually [27], starting from using an electric field, to enhance the water transport in nanochannels and gas dissolving in aqueous solutions [28, 29], to the application of terahertz-regulated dissolution of methane hydrate [30] or using THz wave to detect different materials and defects [31, 32]. Furthermore, in a biological system, THz stimuli can be applied to enhance the permeability of ion channels by directional interaction with functional groups [33–35] and even can be used to accelerate the DNA unwinding [36]. Biophotons at high-frequency THz range can also participate in the replication of DNA and neurotransmission [37, 38]. Previous research on THz–water interaction proves that THz wave can enhance the water permeability by changing the H-bond structure of one-dimensional (1D) and two-dimensional (2D) water in artificial membrane materials such as graphene and carbon tube [39–44]. As a 2D material sharing analogous behaviors with biological membranes, functional groups on GO membranes can also be stimulated with THz EM with high efficiency and directionally [45]. Inspired by the studies of THz light enhancing water transportation by interacting with matter and functional groups, we propose a light-based modulation method targeting edge functional groups to change the permeability of the GO membrane.

In this study, based on a special GO membrane model and primarily considering carboxyl groups on the edge of the membrane (Figure 1A), we uncovered the interaction between 44.0 THz EM wave and carboxyl, as well as the subsequent influence on the conformation of GO membrane water channels. The underlying mechanism is shown to be that THz EM stimuli can change the oscillation of carboxyl at the entrance and exit of the channel by affecting the carboxyl groups resonantly, thereby reducing the energy barrier for water molecules to enter and exit the GO membrane, thus improving the permeability of GO membranes by nearly five times.

Method

To explore the influence of THz EM stimulus on the dynamic properties of edge functional groups on a membrane and its subsequent effect on the conformation of the water channel and the permeability of the membrane, we designed a GO membrane model by stacking two sheets of GO in parallel with lengths, widths, and interlayer spacings of 3.42, 4.94, and 0.78 nm, respectively. Conventionally, the molecular structure of GO contains hydroxyl and epoxy functional groups on the basal plane and carboxyl grafted on the edges of the sheet, following the well-known Lerf–Klinowski model [46]. In our previous research, we studied the effect of the interaction between light and hydroxyl groups on the permeability of the GO membrane, while the epoxy shares a similar property with hydroxyl [45]. Relatively, the location of carboxyl groups exerts its effect on water permeation different from that of hydroxyl and epoxy groups, but it is an ideal model for studying the influence of edge functional groups on water permeation. Therefore, we focused on a pure carboxyl-functionalized GO membrane model to simplify the molecular dynamic simulation and the following data analysis. In order to

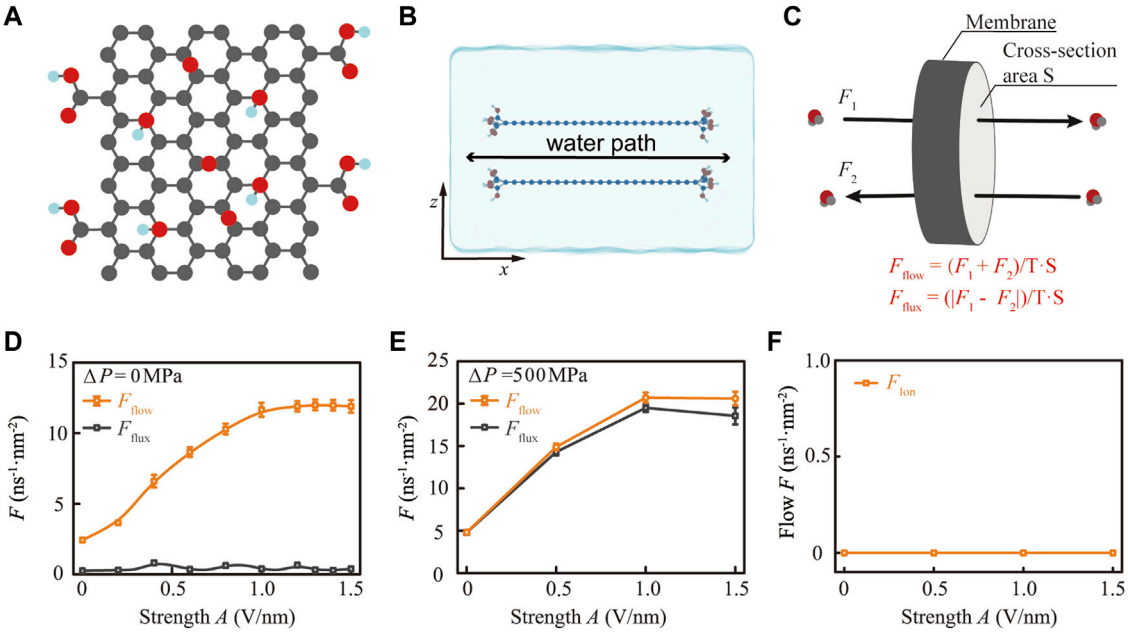

FIGURE 1
Electromagnetic (EM) stimulus at a specific frequency significantly enhances the permeability of the functionalized membrane for water. **(A)** Structural model of the normal GO plate. The gray, red, and cyan balls represent carbon, oxygen, and hydrogen atoms, respectively. **(B)** Schematic diagram of the GO membrane model by stacking two sheets of GO in parallel. **(C)** Schematic diagram for distinguishing water flow and flux, where flow and flux are the sum and difference of water molecules between the forward transport (F_1) and the backward transport (F_2), respectively. **(D)** Transition to a super permeation state of confined water modulated by 44.0 THz EM stimuli (orange curve) at different strengths (A) without the gradient field. **(E)** In the presence of a gradient field with a 500 MPa pressure difference, 44.0 THz EM stimulus enhances both the water flow and flux through the GO membrane. **(F)** EM stimulus did not enhance the permeability of ions due to the steric effect.

ensure that the water can be affected by the carboxyl on the path of permeating through the GO membrane, we grafted the carboxyl at the edge of the GO sheet with a certain space around 0.4–0.8 nm. The charge model for carboxyl was based on the carboxyl group in ASPH amino acid to ensure that the system was electrically neutral. The GO membrane was centered in the simulation box with side lengths of L_x = 5.75 nm, L_y = 5.11 nm, and L_z = 3.78 nm. Then, we filled the rest of the box with flexible SPCE-modelled water molecules [47–49]. Consequently, the size of the GO membrane model and the box ensures that the water molecules can only permeate through the GO membrane along the *x*-axis (Figure 1B; Supplementary Figure S1).

EM waves will be applied to the entire system at the beginning of the MD simulation. Since the electric component of EM waves dominates the interaction of the EM wave with small molecules at room temperature [40], an electric field $\boldsymbol{E}(t) = A \cdot \boldsymbol{u} \cdot \cos(\omega t + \varphi)$ was applied to simulate the EM wave, where A is the maximum amplitude of the electric field that determines the strength of the EM wave. The polarization direction of the wave was set to $\boldsymbol{u}$ = (1, 0, 0), which is parallel to the membrane plane. The frequency f of the EM wave relates to the angular frequency ω *via* the equation $f = \omega/2\pi$. Furthermore, to investigate the effect of hydrostatic pressure and THz stimuli together on the permeability of the membrane, we used the accelerated function of GROMACS to generate desired pressure difference (ΔP) [50]. F was applied to define the permeability of the GO membrane (Figure 1C), where F_1 and F_2 are the number of water molecules traversing forward and backward from one side of the membrane to the other along the *x*-axis, respectively. Furthermore, F_{flow} and F_{flux} are the sum and difference of F_1 and F_2 divided by the product of the simulation time and the cross-section area of the channel, respectively. Therefore, we use F_{flow} to describe the bidirectional permeability and F_{flux} to describe the unidirectional permeability of the membrane. To minimize the influence of temperature fluctuation on the simulation, a Nose–Hoover thermostat with a time constant for coupling of 0.2 ps was applied to maintain the average system temperature at 300 K with a fluctuation under 5 K (Supplementary Figure S2). More details of the simulation methods are shown in Supplementary Section S1.

Result and discussion

Under the effect of 44.0 THz EM, the GO membrane becomes more permeable to water molecules, but repellency to ions is maintained (Figures 1D–F). Evidently, the F_{flow} tends to increase non-linearly with increasing EM stimuli strength A under an equilibrium state, while the F_{flux} only fluctuates within a certain value without a substantial increase (Figure 1D). Under normal conditions without osmotic pressure and THz EM stimuli, the value of the F_{flow} and F_{flux} is around 2.42 ± 0.09 $\mathrm{ns^{-1}{\cdot}nm^{-2}}$ and 0.25 ± 0.01 $\mathrm{ns^{-1}{\cdot}nm^{-2}}$, respectively. With the stimuli of 44.0 THz EM, the F_{flow} will increase rapidly as A increases from 0.1 to 1.0 V/nm and remain in a super state with F_{flow} = 11.89 ± 0.44 $\mathrm{ns^{-1}{\cdot}nm^{-2}}$ when $A \geq$ 1.0 V/nm. In contrast, the F_{flux} fluctuated between 0.25 $\mathrm{ns^{-1}{\cdot}nm^{-2}}$ and 0.65 $\mathrm{ns^{-1}{\cdot}nm^{-2}}$ and does not increase with the stimulation of 44.0 THz EM. The reason behind this fact is that the values of F_1 and F_2 are close to each other under normal conditions, while the THz EM stimuli will boost up both F_1 and F_2, resulting in F_{flux} fluctuating within a certain range. However, if we applied 44.0 THz EM stimuli under a gradient field of ΔP = 500 MPa, both F_{flow} and F_{flux} will be excited to a super permeation state (Figure 1E). This is because the gradient field of ΔP = 500 MPa will boost up F_1 or F_2 depending on the direction of osmotic pressure, leading to a huge diverse between F_1 and F_2; thus, the value of F_{flow} and F_{flux} will be close to each other. Consequently, in the absence of THz EM stimuli, the osmotic pressure of ΔP = 500 MPa can enhance the permeability of the membrane in both F_{flow} and F_{flux} to 4.81 ± 0.31 $\mathrm{ns^{-1}{\cdot}nm^{-2}}$ and 4.78 ± 0.29 $\mathrm{ns^{-1}{\cdot}nm^{-2}}$, respectively. Subsequently, both F_{flow} and F_{flux} can increase by about four times under the stimulation of 44.0 THz EM with strength $A \geq$ 1.0 V/nm, reaching the values of F_{flow} = 20.60 ± 0.99 $\mathrm{ns^{-1}{\cdot}nm^{-2}}$ and F_{flux} = 19.54 ± 0.91 $\mathrm{ns^{-1}{\cdot}nm^{-2}}$. This fact indicates that THz EM stimuli can enhance both the bidirectional and unidirectional permeability of the membrane with the presence of a gradient field.

Notably, we used higher osmotic pressure to make the phenomena more obvious. However, similar phenomena will occur in a lower gradient field, such as ΔP = 50 MPa (see details in Supplementary Figure S3; Supplementary Section S2). Neither gradient field nor THz EM can change the ion rejection of the membrane (Figure 1F). The GO membrane with an interlayer spacing of 0.78 nm has a strong steric effect on ions, which can refuse ions to enter the channel, as F_{Ion} remained 0 $\mathrm{ns^{-1}{\cdot}nm^{-2}}$ at any stimuli strength A. In other words, 44.0 THz EM stimuli can enhance the water permeability of the membrane while keeping the ion rejection of the membrane unchanged.

In order to reveal the mechanism behind the phenomenon of the specific frequency of EM stimuli that can enhance the permeability of functionalized membranes, we focused on the vibration spectrum of carboxyl groups, which are essential for the permeation of water through the membranes. In the classical approximation, the absorption spectrum intensity (I) in terms of frequency can be calculated by using Fourier transform for the autocorrelation function of total charge current $\boldsymbol{J}(t) = \sum_i q_i \boldsymbol{v_i}(t)$ [44], where q_i and $\boldsymbol{v_i}$ represent the charge and velocity of the ith atom, respectively. The first principle of frequency selection is that the stimulation at a particular frequency can resonate with the vibration of functional groups on the membrane (see the frequency selection of other membrane models in Supplementary Figure S4). Furthermore, the stimulation at the selected frequency is weakly absorbed by the bulk water and confined water. As shown in Figure 2A, the carboxyl groups have characteristic peaks at 35.0 THz, 44.0 THz, and 112.0 THz, which correspond to the bending vibration of O-H and the stretching vibrations of C-O and O-H, respectively. They are far away from the prominent absorption peaks of bulk water and confined water, denoting that carboxyl can resonantly absorb the photon energy from the 35.0, 44.0, and 112.0 THz EM stimuli. The vibration modes of C-O and C=O show certain similarities.

To clarify the belonging of the frequency of 44.0 THz, we calculated the vibration of C-O and C=O separately and found out that the vibration of 44.0 THz is mainly contributed to the C-O stretching (Figure 2B). It is essentially in agreement with the result from the FT-IR measurement, indicating that the simulations are well calibrated. Among these characteristic frequencies, only 35.0 and 44.0 THz EM stimuli are able to enhance the permeability of the GO membrane, and the mechanism behind this enhancement is similar (the effect of 35.0 THz EM stimuli on the permeability of the membrane is shown in Supplementary Figure S5; Supplementary Section S4). Therefore, we will focus on 44.0 THz EM stimuli to uncover the mechanism behind this enhancement. From Figure 2C,

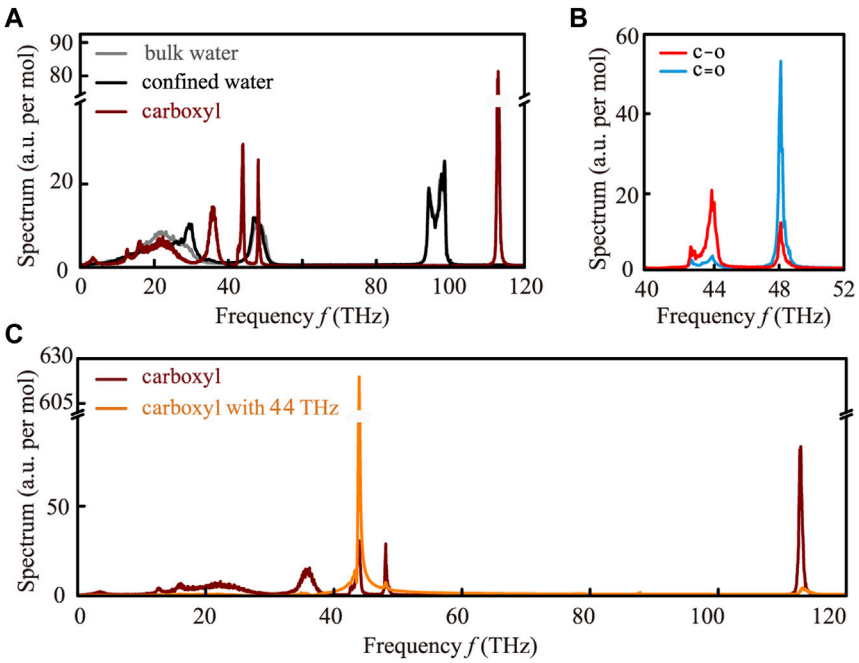

FIGURE 2
Mechanism behind the permeability enhancement of the membrane caused by EM stimuli at a specific frequency. **(A)** Vibrational spectra of bulk water (gray curve), confined water (black curve), and the carboxyl groups on the GO membrane (dark red curve). The vibrational models of carboxyl have characteristic frequencies centered at 35.0, 44.0, and 112.0 THz, respectively, which are far away from the prominent absorption peaks of bulk and confined waters. Consequently, carboxyl resonantly absorbs the photon energy of 35.0 and 44.0 THz EM stimuli, and its dynamical conformation is affected. **(B)** Composition detail of the vibrational spectra of carboxyl at the range of 40.0–52.0 THz. Distinctly, the vibration mode at 44.0 THz is mainly affected by the stretching vibration of the C-O bond. **(C)** Vibrational spectra of the carboxyl group before (dark red curve) and after (orange curve) the application of 44.0 THz stimulus.

we can clearly see that the vibration mode of the carboxyl group changes greatly after the application of 44.0 THz EM stimuli. Notably, the vibration mode with an intrinsic frequency of 44.0 THz is greatly enhanced by the corresponding stimuli, while other vibration modes had been reduced to a relatively weak state. In other words, due to the over-damping phenomenon caused by EM stimuli, all other vibration modes of carboxyl are suppressed, except for the vibration mode with an intrinsic frequency of 44.0 THz. As a result, the motion of the carboxyl group at the entrance of the water channel has changed dramatically under the influence of EM wave stimulation, which undoubtedly changes the permeability of the GO membrane.

Since the carboxyl group is located at the edge of the GO membrane and is hydrophilic, it tends to oscillate up and down in the direction perpendicular to the membrane plane under the attraction of water molecules around and the restriction of the carbon plate (Figure 3A). Figure 3B shows the trajectory of carboxyl in the absence and presence of THz EM stimuli. Evidently, the tendency of carboxyl to oscillate up and down has been suppressed after the application of 44 THz EM, confirming the conclusion of Figure 2C, and all vibration modes except C-O stretching have become weaker. Moreover, we can find that the oscillation period of carboxyl increases with the growth of the EM stimuli strength A (Figure 3C). Originally, it only takes 2.8 ns on average for carboxyl to complete a period of oscillating up and down, but as the stimuli strength A increases to 1.5 V/nm, the oscillation period increased to 8.6 ns on average. The dynamical change in carboxyl also changes the energy barrier for water molecules to permeate through the GO membrane. From Figure 3D, we can see the intermolecular interaction energy between the water molecule and the GO membrane. As the gateway for water molecules permeating through the membrane, carboxyl locates around 1.3 nm and 4.5 nm along the x-axis. Under normal circumstances, hydrophilic carboxyl will attract water molecules by forming H-bond with the interaction energy of $E_{w\text{-}c}$ = -24.0 kJ/mol, making it difficult for water molecules to enter or exit from the inside of the membrane. However, with the application of 44.0 THz EM stimuli, the dynamic conformation of carboxyl changes and the interaction energy $E_{w\text{-}c}$ reduces to -19.0 kJ/mol, making it less attractive to water and easier for water molecules to pass through. This fact leads to the conclusion that the movement change of carboxyl has a great influence on the membrane permeability due to its gateway location of water molecule transportation.

At last, it is worth noting that at the macroscopic level, the electric field required in an experiment to produce the dielectric breakdown of water is 0.07 V/nm. However, in classical molecular dynamics simulations, the electric field needed to affect the dynamic property of water significantly is almost 10 times greater than 0.07 V/nm. We did not observe the dielectric breakdown phenomenon in the simulation because the classical force field fixed the charge of atoms. This treatment just considered the orientation polarization and ignored the electron polarization. At the molecular level, dielectric breakdown is a bond-breaking process [51], and the electric field threshold to dissociate water molecules and sustain an ionic current

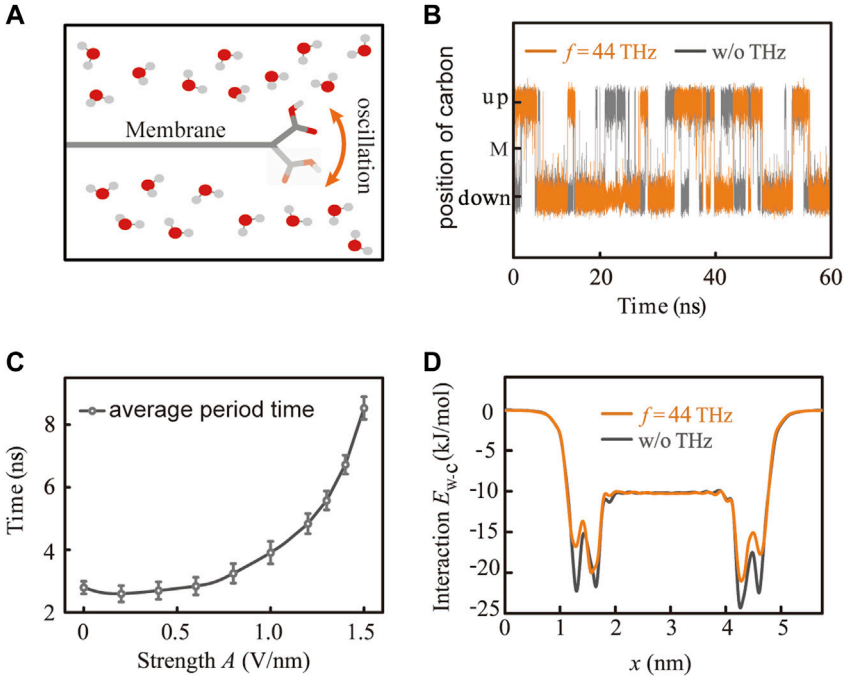

FIGURE 3
Effects of EM stimuli at the specific frequency on the movement of carboxyl. **(A)** Schematic diagram of movement for carboxyl on the edge of the membrane. **(B)** Dynamical conformation of carboxyl before (gray line) and after (orange line) the application of 44.0 THz stimuli, where the label M in the middle of the vertical axis represents the carbon plane of the GO membrane. **(C)** Average period time for the conformational change of carboxyl increases with the growth of stimuli strength of 44.0 THz.**(D)** Interaction energy $E_{w\text{-}c}$ between a water molecule and the membrane along the pathway of water molecules permeating through the membrane.

needs to be up to 3.5 V/nm [52]. Therefore, under this threshold, we can reveal the classical image rather than the quantum image of the influence of the external field on molecular orientation and vibration dynamics. Furthermore, in the simulation, thermal dissipation is based on the thermostat algorithm, while the water bath is used to control the system's temperature in the experiment. Although 44.0 THz is not the strongest absorption frequency band that water absorbs the EM stimulus, the local temperature will still rise if we irradiate the light on the water. Based on the continuous light source we applied in the simulation, the injected power from 44.0 THz EM stimulus to the unit volume of water is less than 0.6×10^{-9} W/nm^3 when $A < 1.5$ V/nm (see details in Supplementary Section S5). Therefore, to investigate the non-thermal effect of the enhancement of membrane permeability caused by light, the water bath needs to be designed to take away the injected energy in the process of the experiment as shown in the previous work [35].

Conclusion

In this work, we found that EM stimuli at a frequency of 44 THz can be resonantly absorbed by carboxyl groups at the edge position of the GO membrane, thereby changing the vibration mode and dynamic conformation of carboxyl groups. As a result, it reduced the energy barrier of water molecule transport and ultimately increased the permeability of the membrane by five times. It is worth noting that in various biological and artificial particle transport channels and membranes, the edge functional groups play an important role in screening molecules or ions. Therefore, our findings bring new insights into the study of biological channels and artificial membranes and provide a new approach to manipulating the transmembrane transport of water molecules and other particles in life science and industrial applications.

Data availability statement

The original contributions presented in the study are included in the article/Supplementary Material; further inquiries can be directed to the corresponding author.

Author contributions

Conceptualization, ZZ; Validation, LW; Investigation, TS and RH; Writing - original draft, TS; Writing - review and editing, YL and ZZ.

Funding

This work was supported by the National Key Research and Development Program of China (No. 2021YFA1200404), National Natural Science Foundation of China Projects (Nos T2241002, 12204547, and 11904231), and Innovation Laboratory of Terahertz

Biophysics and sponsored by Shanghai Sailing Program (No. 19YF1434100).

Acknowledgments

The authors also acknowledge the supercomputer support from Shanghai Snowlake Technology Co., Ltd.

Conflict of interest

The authors declare that the research was conducted in the absence of any commercial or financial relationships that could be construed as a potential conflict of interest.

Publisher's note

Supplementary material

The Supplementary Material for this article can be found online at: https://www.frontiersin.org/articles/10.3389/fphy.2023.1098170/full#supplementary-material

References

1. Koros WJ, Zhang C. Materials for next-generation molecularly selective synthetic membranes. *Nat Mater* (2017) 16(3):289–97. doi:10.1038/nmat4805

2. Feng L, Wu L, Qu X. New horizons for diagnostics and therapeutic applications of graphene and graphene oxide. *Adv Mater* (2013) 25(2):168–86. doi:10.1002/adma.201203229

3. Van der Bruggen B. Chemical modification of polyethersulfone nanofiltration membranes: A review. *J Appl Polym Sci* (2009) 114(1):630–42. doi:10.1002/app.30578

4. Zhu Y, Murali S, Cai W, Li X, Suk JW, Potts JR, et al. Graphene and graphene oxide: Synthesis, properties, and applications. *Adv Mater* (2010) 22(35):3906–24. doi:10.1002/adma.201001068

5. Dideikin AT, Vul AY. Graphene oxide and derivatives: The place in graphene family. *Front Phys* (2019) 6:149. doi:10.3389/fphy.2018.00149

6. Zhu Z, Guo HK, Jiang XK, Chen Y, Song B, Zhu Y, et al. Reversible hydrophobicity–hydrophilicity transition modulated by surface curvature. *J Phys Chem Lett* (2018) 9(9):2346–52. doi:10.1021/acs.jpclett.8b00749

7. Dreyer DR, Park S, Bielawski CW, Ruoff RS. The chemistry of graphene oxide. *Chem Soc Rev* (2010) 39(1):228–40. doi:10.1039/b917103g

8. Elimelech M, Phillip WA. The future of seawater desalination: Energy, technology, and the environment. *Science* (2011) 333(6043):712–7. doi:10.1126/science.1200488

9. Lonsdale HK. The growth of membrane technology. *J Membr Sci* (1982) 10(2-3):81–181. doi:10.1016/s0376-7388(00)81408-8

10. Li C, Yang J, Zhang L, Li S, Yuan Y, Xiao X, et al. Carbon-based membrane materials and applications in water and wastewater treatment: A review. *Environ Chem Lett* (2021) 19(2):1457–75. doi:10.1007/s10311-020-01112-8

11. Nair RR, Wu HA, Jayaram PN, Grigorieva IV, Geim AK. Unimpeded permeation of water through helium-leak–tight graphene-based membranes. *Science* (2012) 335(6067):442–4. doi:10.1126/science.1211694

12. Chen L, Shi G, Shen J, Peng B, Zhang B, Wang Y, et al. Ion sieving in graphene oxide membranes via cationic control of interlayer spacing. *Nature* (2017) 550(7676):380–3. doi:10.1038/nature24044

13. Han Y, Xu Z, Gao C. Ultrathin graphene nanofiltration membrane for water purification. *Adv Funct Mater* (2013) 23(29):3693–700. doi:10.1002/adfm.201202601

14. Hu M, Mi B. Enabling graphene oxide nanosheets as water separation membranes. *Environ Sci Technol* (2013) 47(8):3715–23. doi:10.1021/es400571g

15. Sun P, Zhu M, Wang K, Zhong M, Wei J, Wu D, et al. Selective ion penetration of graphene oxide membranes. *ACS Nano* (2013) 7(1):428–37. doi:10.1021/nn304471w

16. Devanathan R, Chase-Woods D, Shin Y, Gotthold DW. Molecular dynamics simulations reveal that water diffusion between graphene oxide layers is slow. *Sci Rep* (2016) 6(1):29484–8. doi:10.1038/srep29484

17. Abraham J, Vasu KS, Williams CD, Gopinadhan K, Su Y, Cherian CT, et al. Tunable sieving of ions using graphene oxide membranes. *Nat Nanotechnol* (2017) 12(6):546–50. doi:10.1038/nnano.2017.21

18. Chen B, Jiang H, Liu X, Hu X. Observation and analysis of water transport through graphene oxide interlamination. *J Phys Chem C* (2017) 121(2):1321–8. doi:10.1021/acs.jpcc.6b09753

19. Wei N, Peng X, Xu Z. Understanding water permeation in graphene oxide membranes. *ACS Appl Mater Inter* (2014) 6(8):5877–83. doi:10.1021/am500777b

20. Dai H, Xu Z, Yang X. Water permeation and ion rejection in layer-by-layer stacked graphene oxide nanochannels: A molecular dynamics simulation. *J Phys Chem C* (2016) 120(39):22585–96. doi:10.1021/acs.jpcc.6b05337

21. Liu S. Steric effect: A quantitative description from density functional theory. *J Chem Phys* (2007) 126(24):244103. doi:10.1063/1.2747247

22. Tsirelson VG, Stash AI, Liu S. Quantifying steric effect with experimental electron density. *J Chem Phys* (2010) 133(11):114110. doi:10.1063/1.3492377

23. Chen L, Moon JH, Ma X, Zhang L, Chen Q, Peng R, et al. High performance graphene oxide nanofiltration membrane prepared by electrospraying for wastewater purification. *Carbon* (2018) 130:487–94. doi:10.1016/j.carbon.2018.01.062

24. Liu S, Tong X, Chen Y, Crittenden J. Forward solute transport in forward osmosis using a freestanding graphene oxide membrane. *Environ Sci Technol* (2021) 55(9):6290–8. doi:10.1021/acs.est.0c08135

25. El Meragawi S, Akbari A, Hernandez S, Mirshekarloo MS, Bhattacharyya D, Tanksale A, et al. Enhanced permselective separation of per-fluorooctanoic acid in graphene oxide membranes by a simple PEI modification. *J Mater Chem A* (2020) 8(46):24800–11. doi:10.1039/d0ta06523d

26. Han Y, Jiang Y, Gao C. High-flux graphene oxide nanofiltration membrane intercalated by carbon nanotubes. *Acs Appl Mater Inter* (2015) 7(15):8147–55. doi:10.1021/acsami.5b00986

27. Wang P, Lou J, Fang G, Chang C. Progress on cutting-edge infrared-terahertz Biophysics. *IEEE Trans Microw Theor Tech.* (2022) 70(11):5117–40. doi:10.1109/tmtt.2022.3200333

28. Xie Z, Li Z, Li J, Kou J, Yao J, Fan J. Electric field-induced gas dissolving in aqueous solutions. *J Chem Phys* (2021) 154(2):024705. doi:10.1063/5.0037387

29. Zhang QL, Wu YX, Yang RY, Zhang JL, Wang RF. Effect of the direction of static electric fields on water transport through nanochannels. *Chem Phys Lett* (2021) 762:138139. doi:10.1016/j.cplett.2020.138139

30. Zhi Z, Shao-Dian Y, Tong-Chuan D, Zhao Y, Sun TY, Li YM. THz electromagnetic wave regulated dissolution of methane hydrate. *Acta Phys Sin-ch Ed* (2021) 70(24):248705. doi:10.7498/aps.70.20211779

31. Baxter HW, Worrall AA, Pang J, Chen R, Yang B. Volatile liquid detection by terahertz technologies[J]. *Front Phys* (2021) 9:639151. doi:10.3389/fphy.2021.639151

32. Zhenwei Z, Jing X, Rui J, Yinghong W, Hao G, Siyi H, et al. Terahertz non-destructive testing and imaging of high-voltage cables[J]. *Front Phys* (2022) 10:893145. doi:10.3389/fphy.2022.893145

33. Li Y, Chang C, Zhu Z, Sun L, Fan C. Terahertz wave enhances permeability of the voltage-gated calcium channel. *J Am Chem Soc* (2021) 143(11):4311–8. doi:10.1021/jacs.0c09401

34. Li Y, Zhu Z, Sun L, Xiang Z, Chang C, Fan C. Physicochemical insights on terahertz wave diminished side effects of drugs from slow dissociation. *ACS Nano* (2022) 16(5):8419–26. doi:10.1021/acsnano.2c02952

35. Liu X, Qiao Z, Chai Y, Zhu Z, Wu K, Ji W, et al. Nonthermal and reversible control of neuronal signaling and behavior by midinfrared stimulation. *Proc Natl Acad Sci U.S.A* (2021) 118(10):e2015685118. doi:10.1073/pnas.2015685118

36. Wu K, Qi C, Zhu Z, Wang C, Song B, Chang C. Terahertz wave accelerates DNA unwinding: A molecular dynamics simulation study. *J Phys Chem Lett* (2020) 11(17):7002–8. doi:10.1021/acs.jpclett.0c01850

37. Liu G, Chang C, Qiao Z, Wu K, Zhu Z, Cui G, et al. Myelin sheath as a dielectric waveguide for signal propagation in the mid-infrared to terahertz spectral range. *Adv Funct Mater* (2019) 29(7):1807862. doi:10.1002/adfm.201807862

38. Li N, Peng D, Zhang X, Shu Y, Zhang F, Jiang L, et al. Demonstration of biophoton-driven DNA replication via gold nanoparticle-distance modulated yield oscillation. *Nano Res* (2021) 14(1):40–5. doi:10.1007/s12274-020-2937-z

39. Guo YW, Qin JY, Hu JH, Cao JH, Zhu Z, Wang CL. Molecular rotation-caused autocorrelation behaviors of thermal noise in water. *Nucl Sci.Tech* (2020) 31(6):53–10. doi:10.1007/s41365-020-00767-w

40. Zhu Z, Chen C, Chang C, Song B. Terahertz-light induced structural transition and superpermeation of confined monolayer water. *ACS Photon* (2020) 8(3):781–6. doi:10.1021/acsphotonics.0c01336

41. Zhu J, Li H, Li X, Li J. Regulating evaporation of a water nanofilm by applying a terahertz alternating electric field. *J Chem Phys* (2022) 157(13):134707. doi:10.1063/5.0114551

42. Yang RY, Jiang WZ, Huo PY. Anisotropic energy absorption from mid-infrared laser pulses in constrained water systems. *J Mol Liq* (2022) 366:120286. doi:10.1016/j.molliq.2022.120286

43. Tong-Chuan D, Shao-Jian Y, Yon Z, Sun TY, Li YM, Zhu Z. Relationship between hydrogen bond network dynamics of water and its terahertz spectrum. *Acta Phys Sin-ch Ed* (2021) 70(24):248702. doi:10.7498/aps.70.20211731

44. Zhu Z, Chang C, Shu Y, Song B. Transition to a superpermeation phase of confined water induced by a terahertz electromagnetic wave. *J Phys Chem Lett* (2019) 11(1):256–62. doi:10.1021/acs.jpclett.9b03228

45. Sun T, Zhu Z. Light resonantly enhances the permeability of functionalized membranes. *J Membr Sci* (2022) 662:121026. doi:10.1016/j.memsci.2022.121026

46. Lerf A, He H, Forster M, Klinowski J. Structure of graphite oxide revisited. *J Phys Chem B* (1998) 102(23):4477–82. doi:10.1021/jp9731821

47. Toukan K, Rahman A. Molecular-dynamics study of atomic motions in water. *Phys Rev B* (1985) 31(5):2643–8. doi:10.1103/physrevb.31.2643

48. Berendsen HJC, Postma JPM, van Gunsteren WF, Hermans J. Interaction models for water in relation to protein hydration. In: Pullman B, editor. *Intermolecular forces*. Dordrecht: Reidel (1981). p. 331–342.

49. Berendsen HJC, Grigera JR, Straatsma TP. The missing term in effective pair potentials. *J Phys Chem* (1987) 91(24):6269–71. doi:10.1021/j100308a038

50. Zhu F, Tajkhorshid E, Schulten K. Pressure-induced water transport in membrane channels studied by molecular dynamics. *Biophys J* (2002) 83(1):154–60. doi:10.1016/s0006-3495(02)75157-6

51. Huang Z, Nomura K, Nakano A, Wang J. Molecular dynamics simulations of dielectric breakdown of lunar regolith: Implications for water ice formation on lunar surface. *Geophys Res Lett* (2021) 48(3):e2020GL091681. doi:10.1029/2020gl091681

52. Saitta AM, Saija F, Giaquinta PV. *Ab initio* molecular dynamics study of dissociation of water under an electric field. *Phys Rev Lett* (2012) 108(20):207801. doi:10.1103/physrevlett.108.207801